CLEARED
FOR PUBLIC RELEASE
PL/PA 16 DEC 96

Sensor and Simulation Notes
Note 174

January 1973

A PARAMETRIC STUDY OF A CIRCULAR CYLINDER WITHIN TWO PARALLEL PLATES OF FINITE WIDTH

Soon K. Cho and Chiao-Min Chu
The University of Michigan Radiation Laboratory
Department of Electrical and Computer Engineering
Ann Arbor, Michigan 48105

Abstract

A parametric study of the presence of an infinitely long circular cylinder within two parallel plates of finite width is conducted. The numerical method is used for a special case where the axis of the cylinder is constrained on the center plane between the plates in terms of the impedance factor of the system and charge distribution on the cylinder.

PL 96-0976

I

INTRODUCTION

In this report, for TEM wave propagation, we are concerned with the effect of the presence of an infinitely long circular cylinder placed within two parallel plates of finite width. The geometry of such a system is shown in Fig. 1. As seen in Fig. 1, the y-coordinate of the axis of the cylinder is

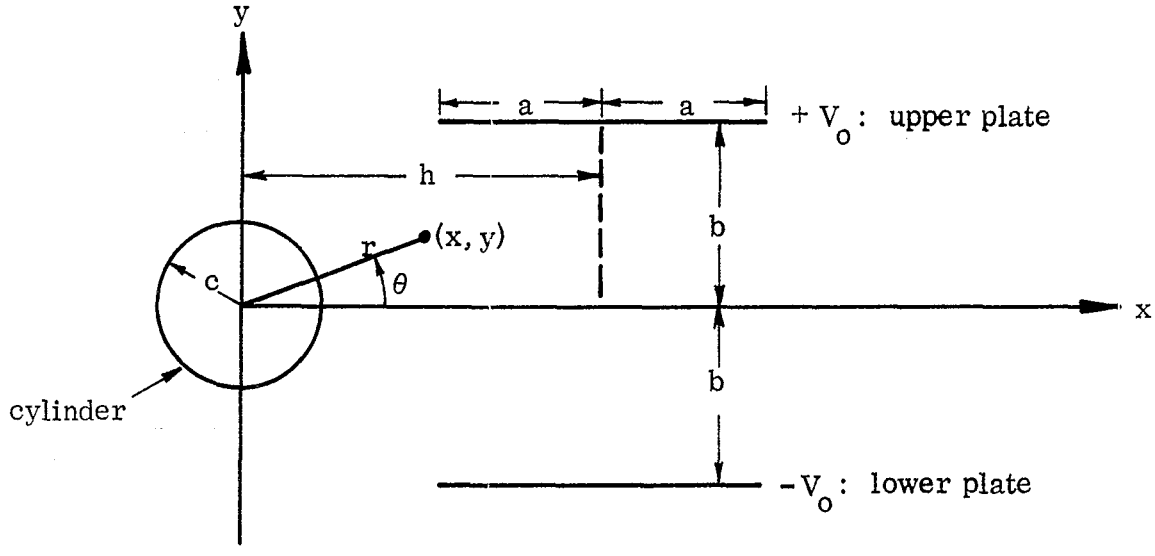

Fig. 1: Geometry of two parallel plates of finite width with a circular cylinder within them.

restricted to be symmetric between the plates.

For a parametric study of the effect of the presence of a circular cylinder, we investigated the impedance factor f_g of the system and the

charge distribution on the cylinder for the following cases of parameters:

(a) for the impedance factor, f_g

$\frac{a}{b} = 0.1,\ 0.2,\ 0.5$ and 1.0,

$\frac{h}{a} = 0,\ 0.2,\ 0.5,\ 1.0$ and 10.0,

$\frac{c}{b} = 0,\ 0.1,\ 0.2,\ 0.3,\ 0.4,\ 0.5,\ 0.6,\ 0.7,\ 0.8,\ 0.9$ and 0.99.

(b) for the charge distribution on the cylinder,

$\frac{a}{b} = 0.1,\ 0.2,\ 0.5$ and 1.0,

$\frac{h}{a} = 0$.

$\frac{c}{b} \leq 0.1,\ 0.5$ and 0.9.

In Section II, mathematical formulations for the impedance factor of the system shown in Fig. 1 and the charge distribution on the circular cylinder are presented. As pointed out at the outset, the y-coordinate of the axis of the cylinder is restricted to the center plane between the plates. The mathematical formulation of the impedance factor for our present system parallels closely that of our previous work[1]. Knowing the charge distribution function of the upper plate, the derivation of the charge on the cylinder is straightforward.

In Section III, numerical results of the impedance factor of our system and the charge distribution on the cylinder are presented both in tabulations and graphs. The graphical presentations are limited for a few representative cases only.

In Section IV, we present some qualitative conclusions for parametric effects of the circular cylinder on the impedance factor of the system and the charge distribution on the cylinder.

II

MATHEMATICAL FORMULATIONS

2.1: Impedance Factor, f_g

For a system shown in Fig. 1, the complex potential of any point (x, y) outside the cylinder is

$$\phi(x,y) + i\,\psi(x,y)$$

$$= \frac{1}{2\pi\epsilon_o} \int_{h-a}^{h+a} dx'\,\sigma(x')\,\mathrm{Ln}\left[\frac{(x+iy-x'+ib)\left(x+iy-\frac{c^2}{x'-ib}\right)}{(x+iy-x'-ib)\left(x+iy-\frac{c^2}{x'+ib}\right)}\right] . \qquad (1)$$

We introduce the coordinate transformation and the normalization of parameters as follows:

$$s = \frac{x'-h}{a} , \qquad (2)$$

$$\xi = \frac{x-h}{a} , \quad \eta = \frac{y-b}{a} , \quad z = \xi + i\eta , \qquad (3)$$

$$B = \frac{2b}{a} , \qquad (4)$$

$$H = \frac{h}{a} , \qquad (5)$$

and

$$C = \frac{c}{a} . \qquad (6)$$

Now, eq. (1) can be written in the following form

$$\frac{2\pi\epsilon_o}{a}\left[\phi(\xi,\eta) + i\psi(\xi,\eta)\right]$$

$$= \int_{-1}^{1} ds\,\sigma(s)\,\mathrm{Ln}\left[\frac{(z-s+iB)\left(s+\hat{\lambda}-i\hat{\nu}\right)\left(s+H+i\frac{B}{2}\right)}{(z-s)\left(s+\hat{\lambda}+iB-i\hat{\nu}\right)\left(s+H-i\frac{B}{2}\right)}\right] , \qquad (7)$$

where

$$\hat{\lambda} = \hat{\lambda}(\xi, \eta) = H - \frac{C^2(z+H)}{(z+H)^2 + (\frac{B}{2})^2} \quad , \tag{8}$$

$$\hat{\nu} = \hat{\nu}(\xi, \eta) = \frac{B}{2}\left[1 - \frac{C^2}{(z+H)^2 + (\frac{B}{2})^2}\right] . \tag{9}$$

Note that the factor $(s+H+i\frac{B}{2})/(s+H-i\frac{B}{2})$ in the integrand of eq. (7) contributes only an imaginary constant and hence may be ignored in the computation.

The mathematical procedure for obtaining the impedance factor for our present system is similar to that in our previous work[1]; therefore, we will simply list the results, omitting the detailed steps involved. Thus,

$$f_{j,k} = (\xi_k - s_j)\,\mathrm{Ln}\left[\frac{|\xi_k - s_j|}{\sqrt{(\xi_k - s_j)^2 + B^2}}\right] + (\lambda_k + s_j)\,\mathrm{Ln}\left[\frac{\sqrt{(\lambda_k + s_j)^2 + \nu_k^2}}{\sqrt{(\lambda_k + s_j)^2 + (B - \nu_k)^2}}\right] + B\left[\tan^{-1}\left(\frac{B}{\xi_k - s_j}\right) + \frac{B-\nu_k}{B}\tan^{-1}\left(\frac{B-\nu_k}{\lambda_k + s_j}\right) - \frac{\nu_k}{B}\tan^{-1}\left(\frac{\nu_k}{\lambda_k + s_j}\right)\right] \tag{10}$$

and

$$g_{j,k} = \frac{\xi_k^2 - s_j^2}{2}\,\mathrm{Ln}\left[\frac{|\xi_k - s_j|}{\sqrt{(\xi_k - s_j)^2 + B^2}}\right] - \frac{\lambda_k^2 - s_j^2}{2}\,\mathrm{Ln}\left[\frac{\sqrt{(\lambda_k + s_j)^2 + \nu_k^2}}{\sqrt{(\lambda_k + s_j)^2 + (B - \nu_k)^2}}\right] + \frac{B^2}{2}\left[\frac{\nu_k}{B} + \mathrm{Ln}\sqrt{(\xi_k - s_j)^2 + B^2}\right]$$

$$+\frac{\nu_k^2}{2}\,\mathrm{Ln}\sqrt{(\lambda_k+s_j)^2+\nu_k^2}\;-\;\frac{(B-\nu_k)^2}{2}\,\mathrm{Ln}\sqrt{(\lambda_k+s_j)^2+(B-\nu_k)^2}$$

$$+B\xi_k\tan^{-1}\left(\frac{B}{\xi_k-s_j}\right)+\lambda_k\nu_k\tan^{-1}\left(\frac{\nu_k}{\lambda_k+s_j}\right)-\lambda_k(B-\nu_k)\tan^{-1}\left(\frac{B-\nu_k}{\nu_k+s_j}\right), \tag{11}$$

where

$$\lambda_k=\hat{\lambda}(\xi_k,0)=H-\frac{C^2(\xi_k+H)}{(\xi_k+H)^2+\left(\frac{B}{2}\right)^2} \tag{12}$$

$$\nu_k=\hat{\nu}(\xi_k,0)=\frac{B}{2}\left[1-\frac{C^2}{(\xi_k+H)^2+\left(\frac{B}{2}\right)^2}\right]\quad. \tag{13}$$

The impedance factor f_g is evaluated by use of eq. (25) in our previous work[1].

2.2: Charge distribution on the circular cylinder

R. W. Latham[2] investigated effects of the presence of a cylinder in two parallel plates of infinite width*.

For our system of Fig. 1, we let

$$x+iy=re^{i\theta} \tag{14}$$

and compute $\frac{\partial}{\partial r}(\phi+i\psi)$ for eq. (1):

$$\frac{\partial\phi}{\partial r}+i\frac{\partial\psi}{\partial r}=\frac{1}{2\pi\epsilon_o}\int_{h-a}^{h+a}dx'\,\sigma(x')\left[\frac{1}{re^{i\theta}-x'+ib}+\frac{1}{re^{i\theta}-\frac{c^2}{x'-ib}}\right.$$

$$\left.-\frac{1}{re^{i\theta}-x'-ib}-\frac{1}{re^{i\theta}-\frac{c^2}{x'+ib}}\right]e^{i\theta}\quad. \tag{15}$$

---

*Our θ differs from that in Ref. (2). For mathematical simplicity, it is convenient in our case to choose the θ-coordinate as shown in Fig. 1.

We now let $r \longrightarrow c$. Noting that $\left.\frac{\partial \psi}{\partial r}\right|_{r=c} = 0$ as it should, we obtain, after some algebraic manipulation*, the charge distribution on the cylinder, $\sigma(\theta)$:

$$\sigma(\theta) = -\left.\frac{\partial \phi}{\partial r}\right|_{r=c} \epsilon_o$$

$$= -\frac{i}{\pi}\int_{-1}^{1} ds\, \sigma(s) \sum_{i=1}^{\infty} C^{n-1}\left[\frac{1}{(s+H+i\frac{B}{2})^n} - \frac{1}{(s+H-i\frac{B}{2})^n}\right] \sin n\theta \,. \tag{16}$$

The charge function $\sigma(\theta)$ can be Fourier-expanded as follows:

$$\sigma(\theta) = \sum_{n=1}^{\infty} A_n \sin n\theta \quad , \tag{17}$$

where

$$A_n = -\frac{i}{\pi}\int_{-1}^{1} ds\, \sigma(s)\left[\frac{1}{(s+H+i\frac{B}{2})^n} - \frac{1}{(s+H-i\frac{B}{2})^n}\right] \,. \tag{18}$$

For a piece-wise linear charge distribution on the plate, $\sigma(s)$, which we assumed to be the case, we obtain

$$A_n = \sum_{j=1}^{2M} \frac{1}{s_{j+1} - s_j}\left\{(\tau_j s_{j+1} - \tau_{j+1} s_j)\left[P_n(s_{j+1}) - P_n(s_j)\right]\right.$$

$$\left. + (\tau_{j+1} - \tau_j)\left[Q_n(s_{j+1}) - Q_n(s_j)\right]\right\}, \tag{19}$$

where

$$P_n(s) = -\frac{i}{\pi} C^{n-1}\int^{s} ds\left[\frac{1}{(s+H+i\frac{B}{2})^n} - \frac{1}{(s+H+i\frac{B}{2})^n}\right] \quad , \tag{20}$$

*In Appendix A, the algebraic steps leading to Eq. (16) are outlined.

$$Q_n(s) = -\frac{i}{\pi} C^{n-1} \int^{s} ds \left[\frac{1}{(s+H+i\frac{B}{2})^n} - \frac{1}{(s+H-i\frac{B}{2})^n} \right] s \quad . \tag{21}$$

Carrying out the integrations for eqs. (20) and (21), one finds

for $n = 1$,
$$P_1(s) = \frac{2}{\pi} \alpha(s) \quad , \tag{22-a}$$

for $n \geq 2$,
$$P_n(s) = \frac{2}{\pi} \frac{1}{n-1} \left(\frac{C}{R(s)}\right)^{n-1} \sin\left[(n-1)\alpha(s)\right] \; ; \tag{22-b}$$

for $n = 1$,
$$Q_1(s) = -\frac{2}{\pi} \left[H\,\alpha(s) + \frac{B}{2} \ell n R(s) \right] \quad , \tag{23-a}$$

for $n = 2$,
$$Q_2(s) = \frac{2C}{\pi} \alpha(s) - \frac{2C}{\pi R(s)} \left[H \sin\alpha(s) - \frac{B}{2} \cos\alpha(s) \right] \quad , \tag{23-b}$$

for $n \geq 3$,
$$Q_n(s) = \frac{2}{\pi} \frac{1}{n-2} \frac{C^{n-1}}{R(s)^{n-2}} \sin\left[(n-2)\,\alpha(s)\right]$$
$$- \frac{2}{\pi} \frac{1}{n-1} \left(\frac{C}{R(s)}\right)^{n-1} \left\{ H \sin\left[(n-1)\,\alpha(s)\right] - \frac{B}{2} \cos\left[(n-1)\,\alpha(s)\right] \right\} , \tag{23-c}$$

where
$$\alpha(s) = \tan^{-1} \frac{B}{2(s+H)} \quad , \tag{24}$$

$$R(s) = \sqrt{(s+H)^2 + (\frac{B}{2})^2} \quad . \tag{25}$$

III

NUMERICAL RESULTS OF IMPEDANCE FACTOR OF THE SYSTEM AND CHARGE DISTRIBUTION ON THE CYLINDER

In Section II, we introduced the normalized parameters B, H and C: $B = 2b/a$, $H = h/a$, $C = c/a$. In practice, it is more convenient to normalize the radius of the cylinder with respect to b, while it is physically more reasonable to normalize the position of the center of the cylinder (i.e., the x-coordinate of the center of the cylinder) with respect to a. For convenient reference, we present in Tables I, II and III, the conversion charts for C, h/b, and B, respectively.

Table I: Conversion Chart for C

c/b \ a/b	0.1	0.2	0.5	1.0
0	0	0	0	0
0.1	1	0.5	0.2	0.1
0.2	2	1.0	0.4	0.2
0.3	3	1.5	0.6	0.3
0.4	4	2.0	0.8	0.4
0.5	5	2.5	1.0	0.5
0.6	6	3.0	1.2	0.6
0.7	7	3.5	1.4	0.7
0.8	8	4.0	1.6	0.8
0.9	9	4.5	1.8	0.9
0.99	9.9	4.95	1.98	0.99

Table II: Conversion Chart for h/b

H \ a/b	0.1	0.2	0.5	1.0
0	0	0	0	0
0.2	0.02	0.04	0.1	0.2
0.5	0.05	0.1	0.25	0.5
1.0	0.1	0.2	0.5	1.0
10.0	1.0	2.0	5.0	10.0

Table III: Conversion Chart for B

a/b	0.1	0.2	0.5	1.0
B	20	10	4	2

As was the case in our previous work[1], it is necessary for us to know the charge distribution on the plate in order to compute the impedance factor of the system. The mathematical procedure for f_g of our present system is formally quite similar to that of the imaged finite parallel plates and was briefly discussed in Section 2.1. As in our previous work[1], we divided the upper plate width into 20 segments and in each segment a linear approximation was made for the charge function.

An examination of preliminary data of f_g indicated that, the the range of h/a, $0 \leq h/a \leq 1.0$, the dependence of f_g on c/b and a/b is more critical than on h/a. As indicated in the Introduction, the numerical computation of the impedance factor, f_g, of the system was carried out for the following cases:

$$\frac{a}{b} = 0.1,\ 0.2,\ 0.5 \text{ and } 1.0,$$

$$\frac{h}{a} = 0,\ 0.2,\ 0.5,\ 1.0 \text{ and } 10.0,$$

$$\frac{c}{b} = 0\ \ 0.1,\ 0.2,\ 0.3,\ 0.4,\ 0.5,\ 0.6,\ 0.7,\ 0.8,\ 0.9 \text{ and } 0.99,$$

and the results are presented in Table IV.

Table IV: Impedance factor, f_g, of two parallel plates

a/b = 0.1

h/a \ c/b	0	0.2	0.5	1.0	10.0
0	1.174366	1.174366	1.174366	1.174366	1.174366
0.1	1.168062	1.168067	1.168093	1.168182	1.172758
0.2	1.149140	1.149159	1.149259	1.149608	1.167839
0.3	1.117491	1.117532	1.117746	1.118502	1.159313
0.4	1.072685	1.072754	1.073118	1.074403	1.146672
0.5	1.013551	1.013656	1.014202	1.016134	1.129170
0.6	0.937401	0.937549	0.938323	0.941059	1.105782
0.7	0.838333	0.838541	0.839625	0.843457	1.075137
0.8	0.702627	0.704521	0.704521	0.710134	1.035383
0.9	0.491631	0.492144	0.494828	0.504272	0.983910
0.99	0.097914	0.098775	0.103422	0.121392	0.924284

a/b = 0.2

h/a \ c/b	0	0.2	0.5	1.0	10.0
0	0.954908	0.954908	0.954908	0.954908	0.954908
0.1	0.948786	0.948804	0.948895	0.949204	0.954648
0.2	0.930410	0.930478	0.930833	0.932041	0.953858
0.3	0.899687	0.899835	0.900600	0.903219	0.952506
0.4	0.856256	0.856506	0.857803	0.862257	0.950539

a/b = 0.2 (continued)

c/b \ h/a	0	0.2	0.5	1.0	10.0
0.5	0.799146	0.799518	0.801452	0.808120	0.947875
0.6	0.726178	0.726696	0.729390	0.738703	0.944403
0.7	0.632813	0.633513	0.637155	0.649779	0.939971
0.8	0.509478	0.510425	0.515361	0.532525	0.934378
0.9	0.333668	0.334965	0.341766	0.365780	0.927360
0.99	0.066840	0.067626	0.072330	0.097912	0.919543

a/b = 0.5

c/b \ h/a	0	0.2	0.5	1.0	10.0
0	0.670940	0.670940	0.670940	0.670940	0.670940
0.1	0.665832	0.665889	0.666179	0.667086	0.670931
0.2	0.650491	0.650713	0.651845	0.655414	0.670901
0.3	0.624850	0.625329	0.627780	0.635593	0.670853
0.4	0.588725	0.589529	0.593662	0.607048	0.670783
0.5	0.541690	0.542859	0.548902	0.568886	0.670694
0.6	0.482869	0.484409	0.492436	0.519726	0.670582
0.7	0.410538	0.412411	0.422295	0.457257	0.670448
0.8	0.321262	0.323338	0.334544	0.377001	0.670290
0.9	0.207082	0.208947	0.219582	0.267424	0.670106
0.99	0.501227	0.051561	0.053861	0.085490	0.669917

$a/b = 1.0$

c/b \ h/a	0	0.2	0.5	1.0	10.0
0	0.472441	0.472441	0.472441	0.472441	0.472441
0.1	0.469161	0.469202	0.469439	0.470389	0.472441
0.2	0.459270	0.459432	0.460364	0.464133	0.472439
0.3	0.442615	0.442967	0.445006	0.453377	0.472436
0.4	0.418922	0.419519	0.422992	0.437594	0.472431
0.5	0.387767	0.388637	0.393738	0.415960	0.472425
0.6	0.348487	0.349616	0.356327	0.387235	0.472418
0.7	0.299953	0.301264	0.309225	0.349317	0.472410
0.8	0.239925	0.241235	0.249491	0.298196	0.472400
0.9	0.162440	0.163395	0.223328	0.228828	0.472389
0.99	0.046983	0.047522	0.048281	0.079989	0.472377

In Table IV, $c/b = 0$ corresponds to the case where the cylinder is not present in the two parallel plates of finite width. Such cases were analyzed by Brown and Granzow[3] by a method different from ours*, and some of their results are compared with our present results below.

$\frac{a}{b}$	f_g B-G	f_g C-C	f_g B-G $-$ f_g C-C
0.2	0.95512	0.954908	-0.000212
0.5	0.67116	0.670940	-0.000220
1.0	0.47264	0.472441	-0.000199

*f_g B-C and f_g C-C denote, respectively, the values of f_g by Brown, Granzow and Chu-Cho.

It appears that, by increasing the number of segments into which the upper plate was divided in our numerical scheme, a better agreement between the two sets of impedance factors could be brought about. This could be easily done, if desired, but at a considerably higher expense for running such a computer program.

For a parametric study of the impedance factor, f_g, for the system shown in Fig. 1, we define Δf_g:

$$\Delta f_g = f_g - f_{g_o} ,$$

where f_{g_o} denotes the impedance factor of two parallel plates of finite width without the presence of a circular cylinder.

In Table V, Δf_g are tabulated to see the dependence of Δf_g on c/b and h/a with a/b as a parameter.

Table V: Dependence of Δf_g on c/b, h/a with a/b as a parameter

a/b = 0.1

c/b \ h/a	0	0.2	0.5	1.0	10.0
0.1	-0.006304	-0.006299	-0.006273	-0.006184	-0.001608
0.2	-0.025226	-0.025209	-0.025107	-0.024758	-0.006527
0.3	-0.056875	-0.056834	-0.056620	-0.055864	-0.015053
0.4	-0.101681	-0.101612	-0.101248	-0.099963	-0.027694
0.5	-0.160815	-0.160710	-0.160164	-0.158232	-0.045196
0.6	-0.236965	-0.236817	-0.236043	-0.233307	-0.068584
0.7	-0.336033	-0.335825	-0.334741	-0.330909	-0.099229
0.8	-0.471739	-0.471435	-0.469845	-0.464232	-0.138983
0.9	-0.682735	-0.682222	-0.679538	-0.670094	-0.190456
0.99	-1.086452	-1.075591	-1.070944	-1.052974	-0.250084

$a/b = 0.2$

h/a / a/b	0	0.2	0.5	1.0	10.0
0.1	-0.006122	-0.006104	-0.006013	-0.005704	-0.000260
0.2	-0.024498	-0.024430	-0.024075	-0.022867	-0.001050
0.3	-0.055221	-0.055073	-0.054308	-0.051689	-0.002402
0.4	-0.098652	-0.098402	-0.097105	-0.092651	-0.004369
0.5	-0.155762	-0.155390	-0.153456	-0.146788	-0.007033
0.6	-0.228730	-0.228312	-0.225518	-0.216205	-0.010505
0.7	-0.322095	-0.321395	-0.327753	-0.305129	-0.014937
0.8	-0.445430	-0.444473	-0.439547	-0.422383	-0.020530
0.9	-0.621240	-0.619943	-0.613142	-0.589128	-0.027548
0.99	-0.888068	-0.887282	-0.882578	-0.856996	-0.035365

$a/b = 0.5$

h/a / c/b	0	0.2	0.5	1.0	10.0
0.1	-0.005108	-0.005051	-0.004761	-0.003854	-0.000009
0.2	-0.020449	-0.020227	-0.019095	-0.015526	-0.000039
0.3	-0.046090	-0.045611	-0.043160	-0.035347	-0.000090
0.4	-0.082215	-0.081411	-0.077278	-0.063892	-0.000157
0.5	-0.129250	-0.128081	-0.122038	-0.112054	-0.000246
0.6	-0.188071	-0.186531	-0.178504	-0.151214	-0.000358
0.7	-0.260402	-0.258529	-0.248645	-0.213683	-0.000492
0.8	-0.349678	-0.347602	-0.336396	-0.293939	-0.000650
0.9	-0.463858	-0.461993	-0.451358	-0.403516	-0.000836
0.99	-0.619712	-0.618379	-0.617079	-0.595450	-0.001023

a/b = 1.0

c/b \ h/a	0	0.2	0.5	1.0	10.0
0.1	-0.003280	-0.003239	-0.003002	-0.002052	0
0.2	-0.01370	-0.013009	-0.012077	-0.008308	-0.000002
0.3	-0.029826	-0.029474	-0.027435	-0.019064	-0.000005
0.4	-0.053519	-0.052922	-0.049449	-0.034847	-0.000010
0.5	-0.084674	-0.083804	-0.078703	-0.056481	-0.000016
0.6	-0.124954	-0.122825	-0.116114	-0.085206	-0.000023
0.7	-0.172488	-0.171177	-0.163216	-0.123124	-0.000031
0.8	-0.232516	-0.231206	-0.222950	-0.174245	-0.000041
0.9	-0.310001	-0.309046	-0.302607	-0.249113	-0.000052
0.99	-0.425458	-0.424919	-0.424160	-0.392452	-0.000064

In order to exhibit more clearly the dependence of Δf_g on a/b and h/a with c/b as a parameter, we rearrange the data in Table V and the results are presented in Table VI.

Table VI: Dependence of Δf_g on a/b and h/a with c/b as a parameter

c/b = 0.1

a/b \ h/a	0	0.2	0.5	1.0	10.0
0.1	-0.006304	-0.006299	-0.006273	-0.006184	-0.001608
0.2	-0.006122	-0.006104	-0.006013	-0.005704	-0.000260
0.5	-0.005108	-0.005051	-0.004761	-0.003854	-0.000009
1.0	-0.003280	-0.003239	-0.003002	-0.002052	0

c/b = 0.2

h/a / a/b	0	0.2	0.5	1.0	10.0
0.1	-0.025226	-0.025209	-0.024107	-0.024758	-0.006527
0.2	-0.024498	-0.024430	-0.024075	-0.022867	-0.001050
0.5	-0.020449	-0.020227	-0.019095	-0.015526	-0.000039
1.0	-0.01370	-0.013009	-0.012077	-0.008308	-0.000002

c/b = 0.3

h/a / a/b	0	0.2 v	0.5	1.0	10.0
0.1	-0.056875	-0.056834	-0.056620	-0.055864	-0.015053
0.2	-0.055221	-0.055073	-0.054308	-0.051689	-0.002402
0.5	-0.046090	-0.045611	-0.043160	-0.035347	-0.000090
1.0	-0.029826	-0.029474	-0.027435	-0.019064	-0.000005

c/b = 0.4

h/a / a/b	0	0.2	0.5	1.0	10.0
0.1	-0.101681	-0.010612	-0.101248	-0.099963	-0.027694
0.2	-0.098652	-0.098402	-0.097105	-0.092651	-0.004369
0.5	-0.102215	-0.081411	-0.077278	-0.063892	-0.000157
1.0	-0.053519	-0.052922	-0.049449	-0.034847	-0.000010

c/b = 0.5

a/b \ h/a	0	0.2	0.5	1.0	10.0
0.1	-0.160815	-0.160710	-0.160164	-0.158232	-0.045196
0.2	-0.155762	-0.155390	-0.153456	-0.146788	-0.007033
0.5	-0.129850	-0.128081	-0.122038	-0.112054	-0.000246
1.0	-0.084674	-0.083804	-0.078703	-0.056481	-0.000016

c/b = 0.6

a/b \ h/a	0	0.2	0.5	1.0	10.0
0.1	-0.236965	-0.236817	-0.236043	-0.233307	-0.068584
0.2	-0.228730	-0.228312	-0.225518	-0.216205	-0.010505
0.5	-0.188071	-0.186531	-0.178504	-0.151214	-0.000358
1.0	-0.124954	-0.122825	-0.116114	-0.0825206	-0.000023

c/b = 0.7

a/b \ h/a	0	0.2	0.5	1.0	10.0
0.1	-0.336033	-0.335825	-0.334741	-0.330909	-0.099229
0.2	-0.322095	-0.321395	-0.327753	-0.305129	-0.014937
0.5	-0.260402	-0.258529	-0.248645	-0.213683	-0.000492
1.0	-0.172488	-0.171177	-0.163216	-0.123124	-0.000031

c/b = 0.8

a/b \ h/a	0	0.2	0.5	1.0	10.0
0.1	-0.471739	-0.471435	-0.469845	-0.464232	-0.138783
0.2	-0.445430	-0.444473	-0.439547	-0.422383	-0.020530
0.5	-0.349678	-0.347602	-0.336396	-0.293939	-0.000650
1.0	-0.232516	-0.231206	-0.222950	-0.174245	-0.000041

c/b = 0.9

a/b \ h/a	0	0.2	0.5	1.0	10.0
0.1	-0.682735	-0.682222	-0.679538	-0.670094	-0.190456
0.2	-0.621240	-0.619943	-0.613142	-0.589128	-0.027548
0.5	-0.463858	-0.461993	-0.4513586	-0.463516	-0.000836
1.0	-0.310001	-0.309046	-0.302607	-0.249113	-0.000052

c/b = 0.99

a/b \ h/a	0	0.2	0.5	1.0	10.0
0.1	-1.086452	-1.075591	-1.070944	-1.052974	-0.250084
0.2	-0.888068	-0.887282	-0.882578	-0.856996	-0.035365
0.5	-0.619712	-0.618379	-0.617079	-0.595450	-0.001023
1.0	-0.425458	-0.424919	-0.424160	-0.392452	-0.000064

In Figs. 3-1 through 3-4, we present Δf_g as functions of c/b with a/b and b/a as parameters. In Figs. 3-5 through 3-8, Δf_g are shown as functions of a/b with c/b and h/a as parameters; in Figs. 3-9 through 3-12, Δf_g are shown as functions of a/b for each given h/a.

The charge distribution $\sigma(\theta)$ on the circular cylinder is numerically obtained for cases of $\frac{a}{b} = 0.1,\ 0.2,\ 0.5$ and 1.0; $\frac{c}{b} \leq \frac{a}{b}$ with $\frac{h}{a} = 0$ by Fourier expansion in θ (see Fig. 1 for θ). $\sigma(\theta)$ is anti-symmetric about $\theta = 0$ in the θ-domain, $0 \leq \theta \leq 2\pi$ in a general case for $H \neq 0$, and in the domain $-\frac{\pi}{2} \leq \theta \leq \frac{\pi}{2}$ in a special case for $H = 0$.

For the cases of $H = 0$, with which we are concerned in this report, it is easily seen that the terms of even integer in Eq. (17) vanish, so that $\sigma(\theta)$ can be written more explicitly in the form

$$\sigma(\theta) = \sum_{k=1}^{\infty} A_{2k-1} \sin\left[(2k-1)\,\theta\right] \quad .$$

The Fourier coefficients for the cases mentioned above are listed in Table VII. The charge distribution on a circular cylinder within two parallel plates of infinite width was treated by Latham[2]. It is observed that, due to the employment of normalization different from ours, the Fourier coefficient in our work, A_n, is related to that in the work of Latham, C_n, by

$$\left|A_n\right| = \frac{(a/b)}{\pi}\, C_n \quad .$$

A_n for $\frac{a}{b} = 10$, $H = 0$, $\frac{c}{b} = 0.5$ was computed and the result is as shown below:

$$A_1 = -3.488, \quad A_3 = +0.000206 \quad .$$

In terms of C_n, when the difference in θ is taken into account, we get

$$C_1 = 1.252, \quad C_3 = 0.00006 \quad ,$$

indicating that, although the leading term agrees fairly closely, the convergence of Fourier expansion for the case of finite width, $\frac{a}{b} = 10$ is much more rapid than that for the case of infinite width.

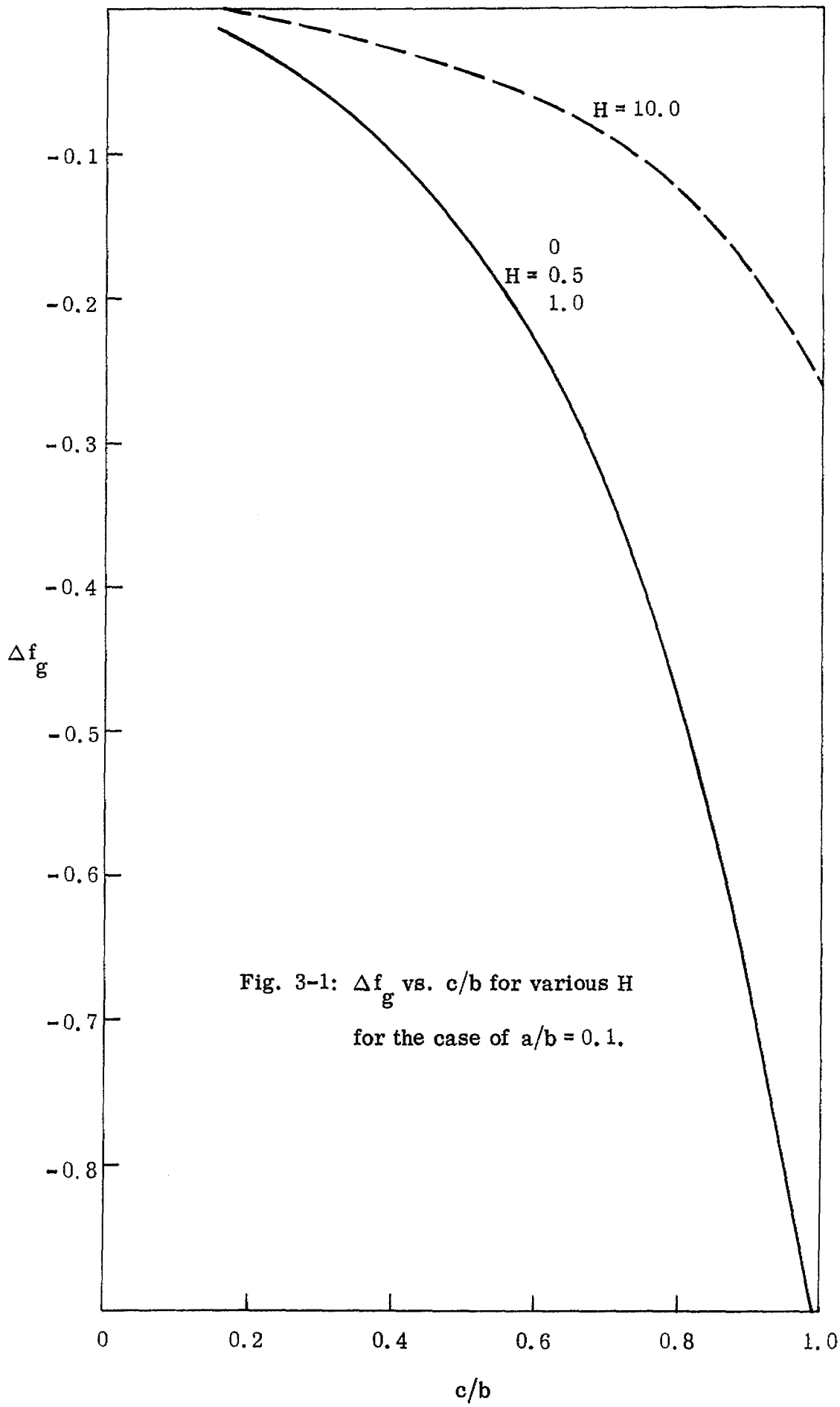

Fig. 3-1: Δf_g vs. c/b for various H for the case of a/b = 0.1.

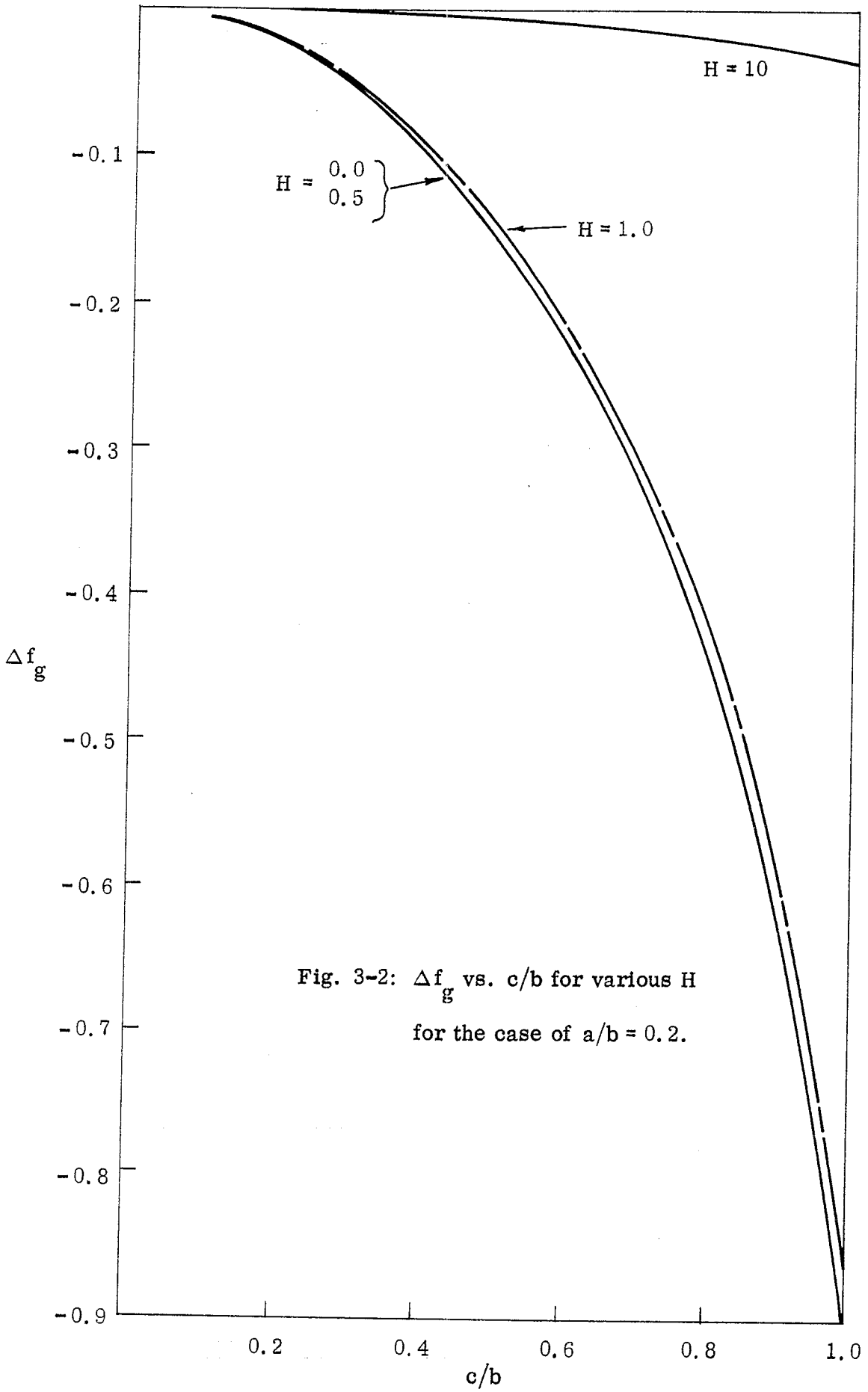

Fig. 3-2: Δf_g vs. c/b for various H for the case of a/b = 0.2.

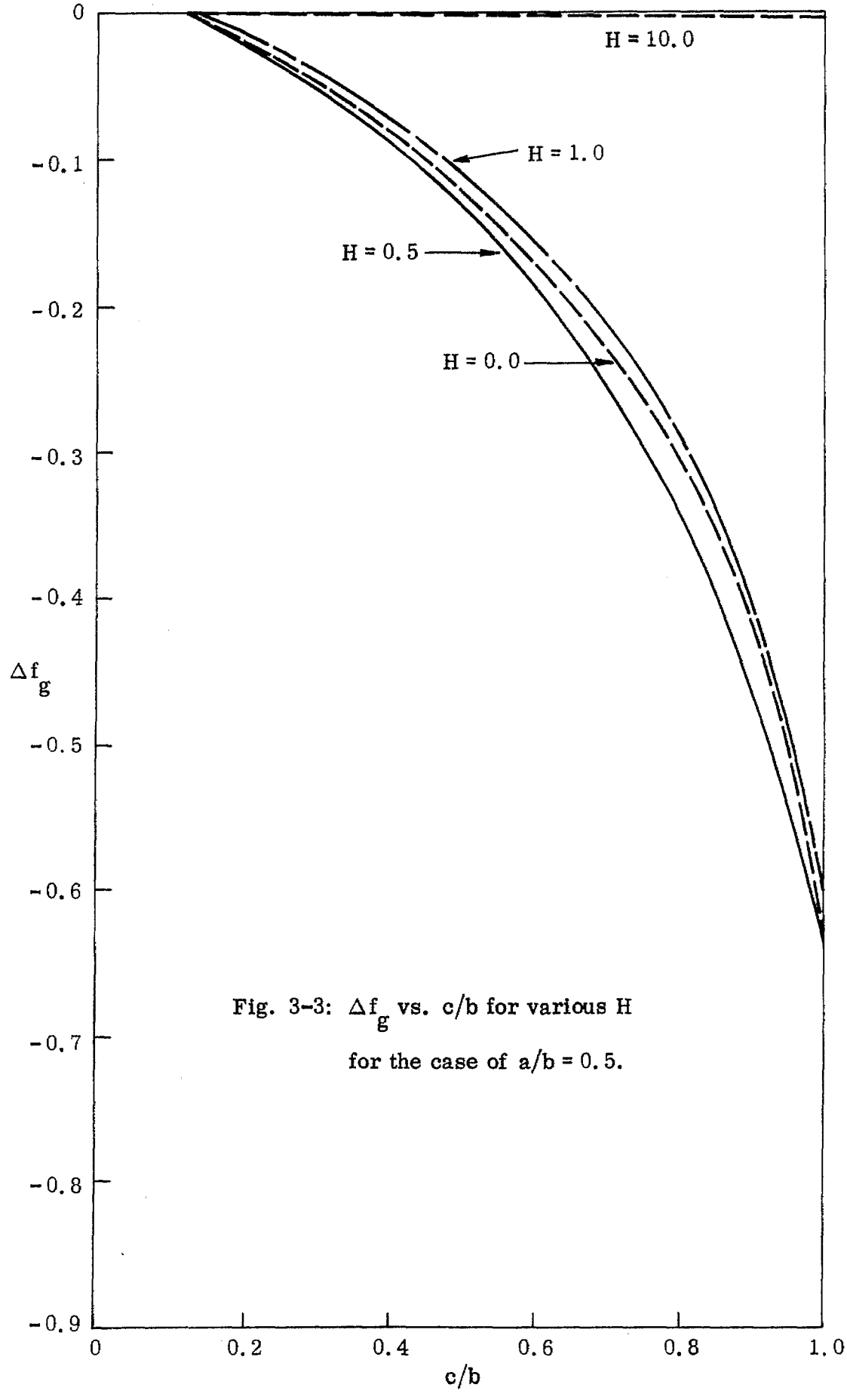

Fig. 3-3: Δf_g vs. c/b for various H for the case of a/b = 0.5.

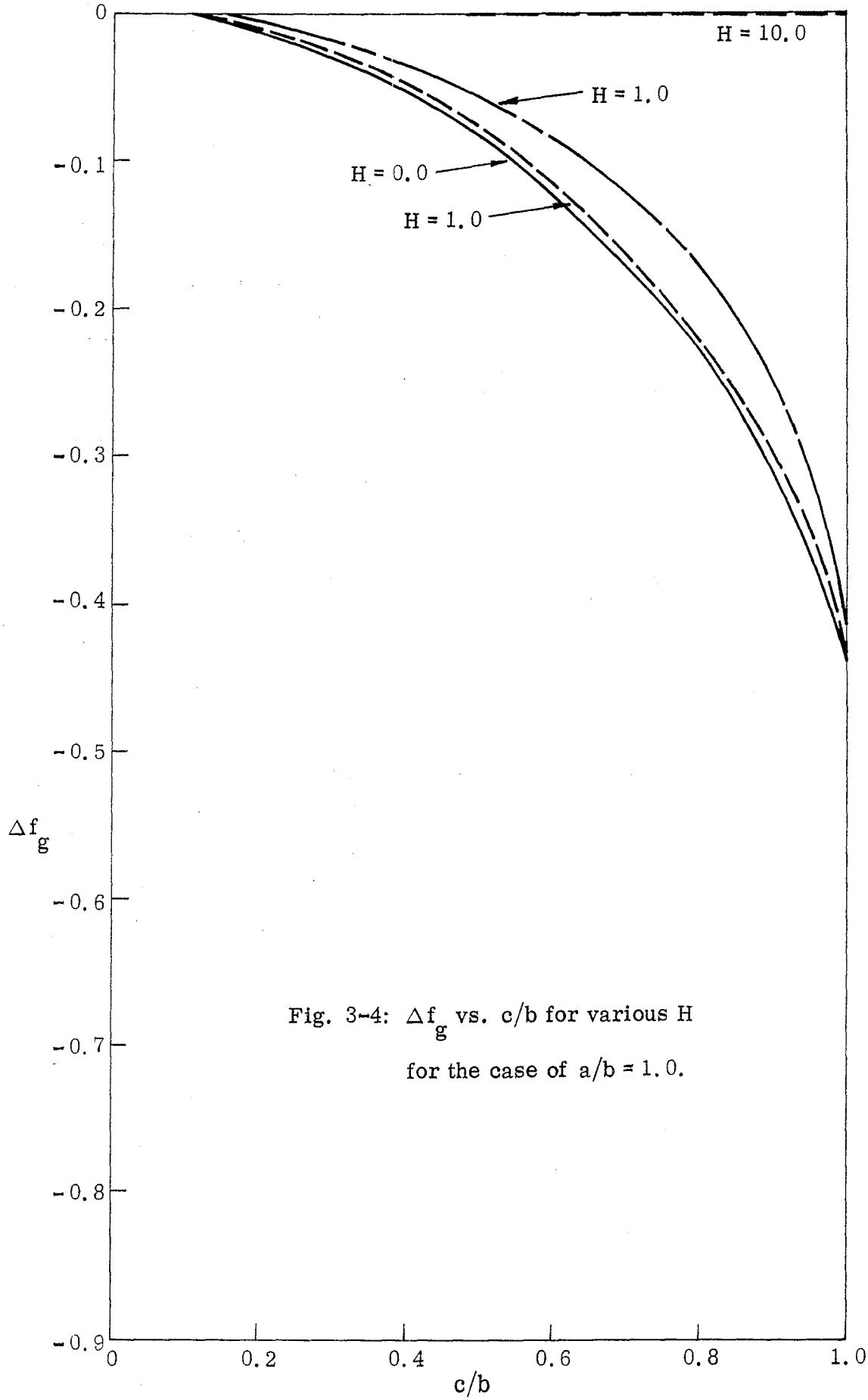

Fig. 3-4: Δf_g vs. c/b for various H for the case of a/b = 1.0.

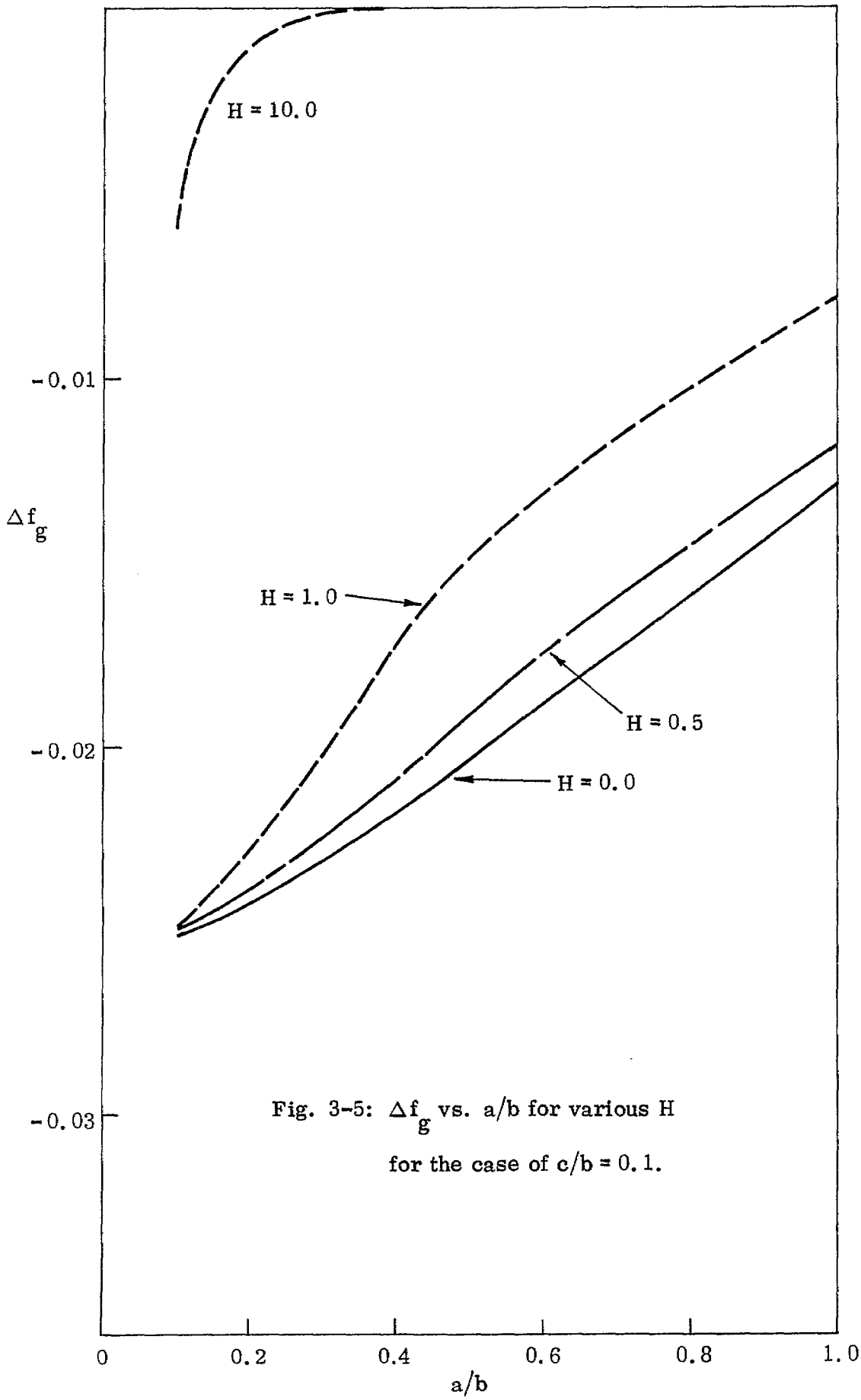

Fig. 3-5: Δf_g vs. a/b for various H for the case of c/b = 0.1.

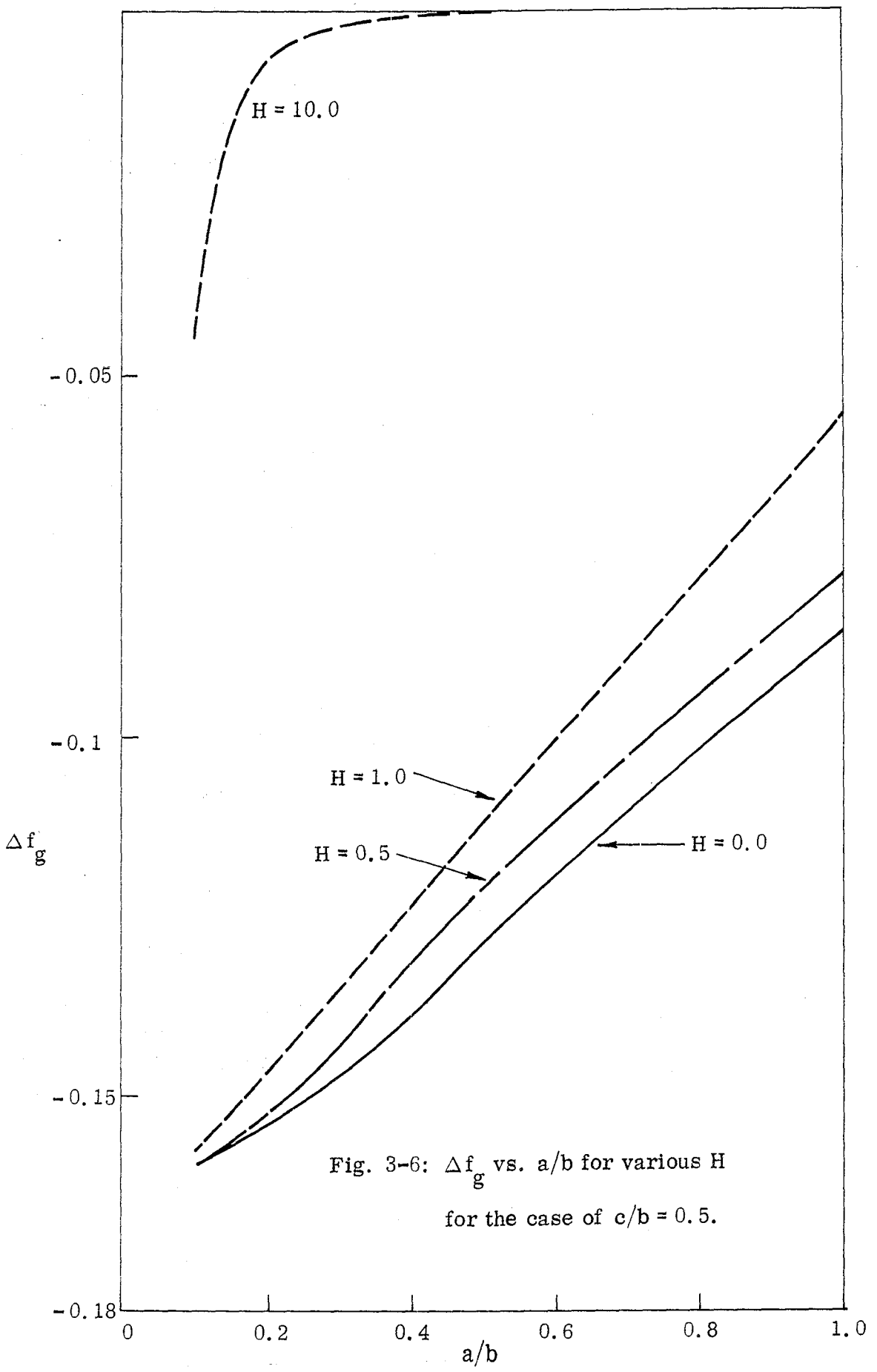

Fig. 3-6: Δf_g vs. a/b for various H for the case of c/b = 0.5.

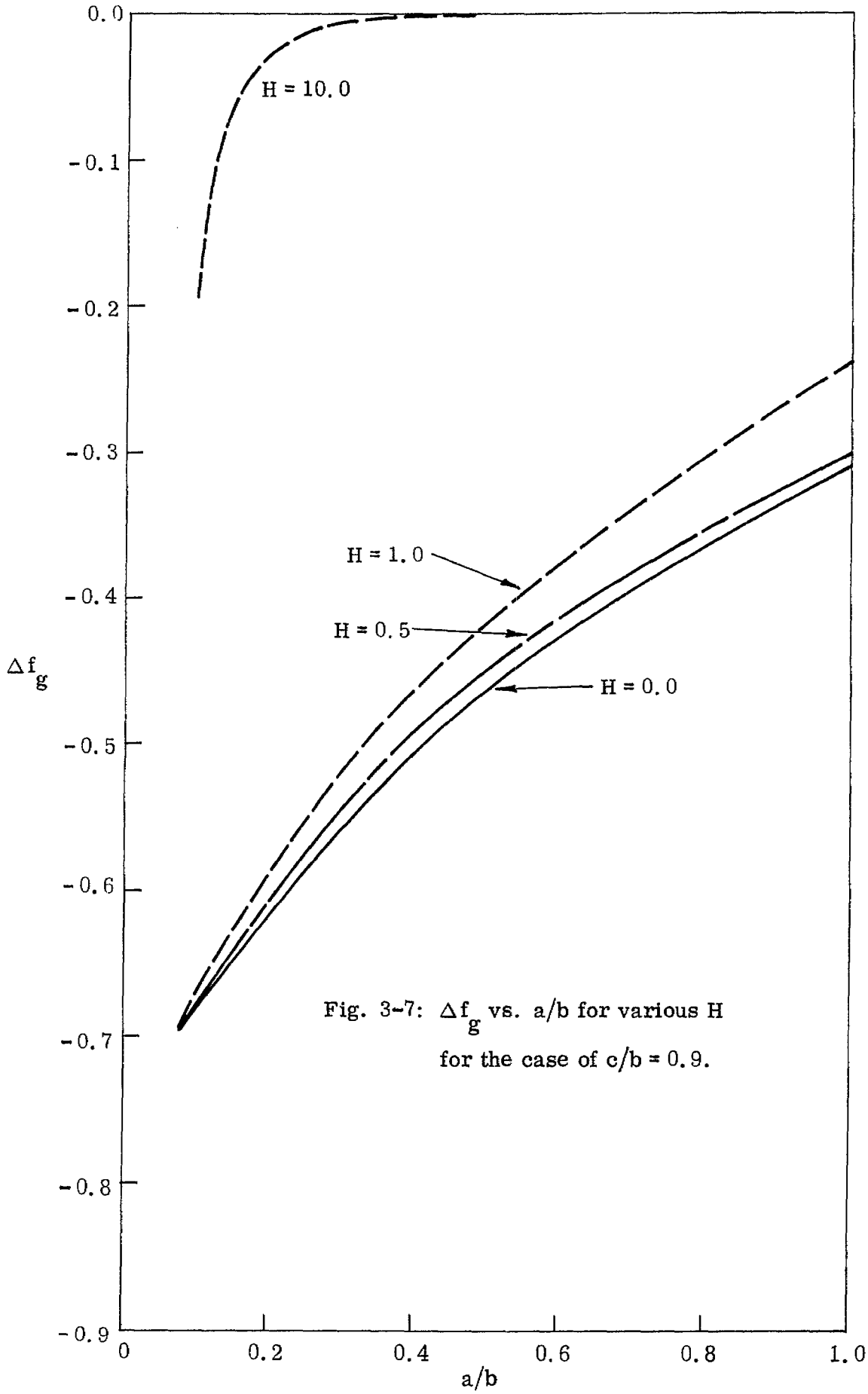

Fig. 3-7: Δf_g vs. a/b for various H for the case of c/b = 0.9.

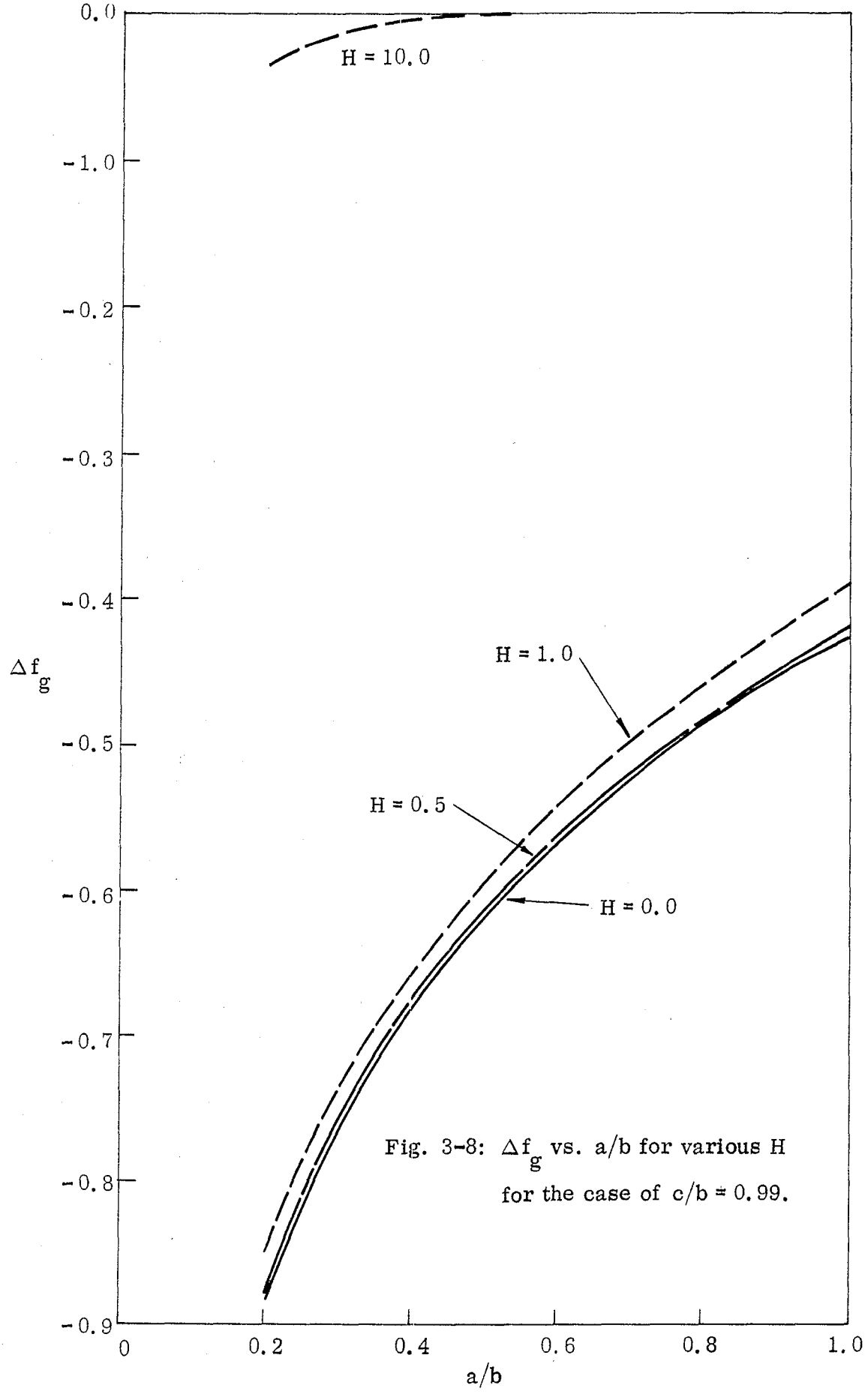

Fig. 3-8: Δf_g vs. a/b for various H for the case of c/b = 0.99.

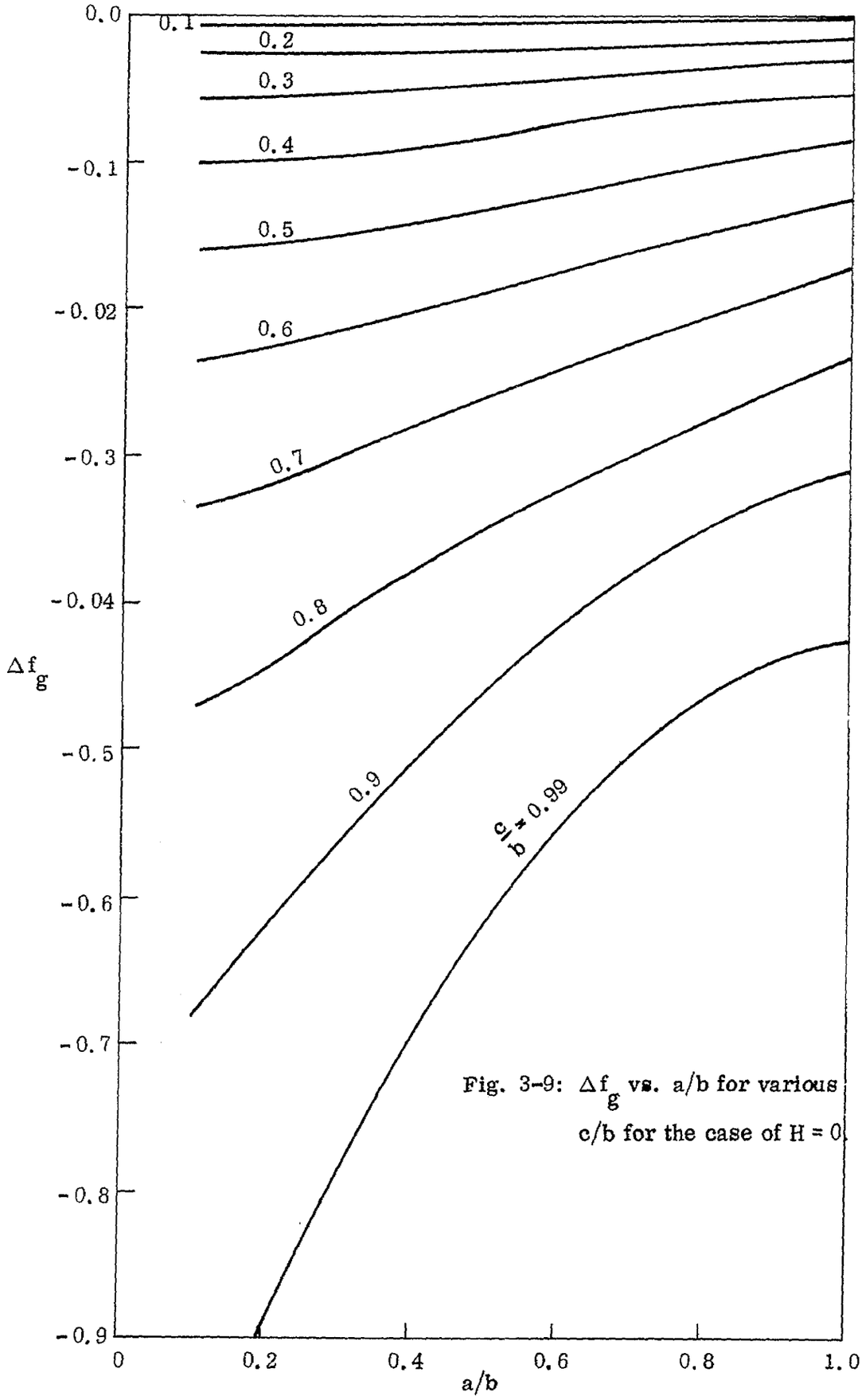

Fig. 3-9: Δf_g vs. a/b for various c/b for the case of H = 0.

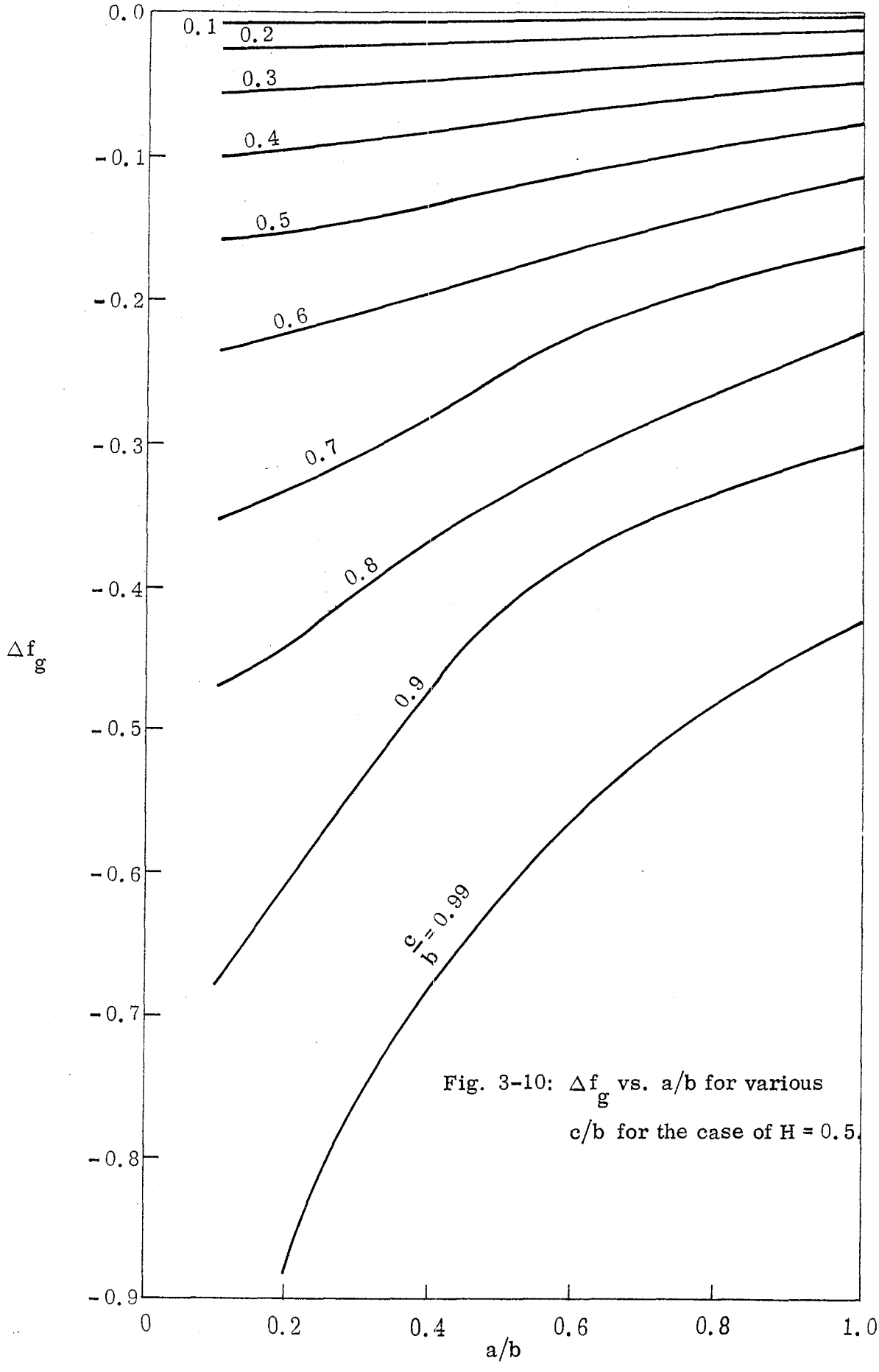

Fig. 3-10: Δf_g vs. a/b for various c/b for the case of H = 0.5.

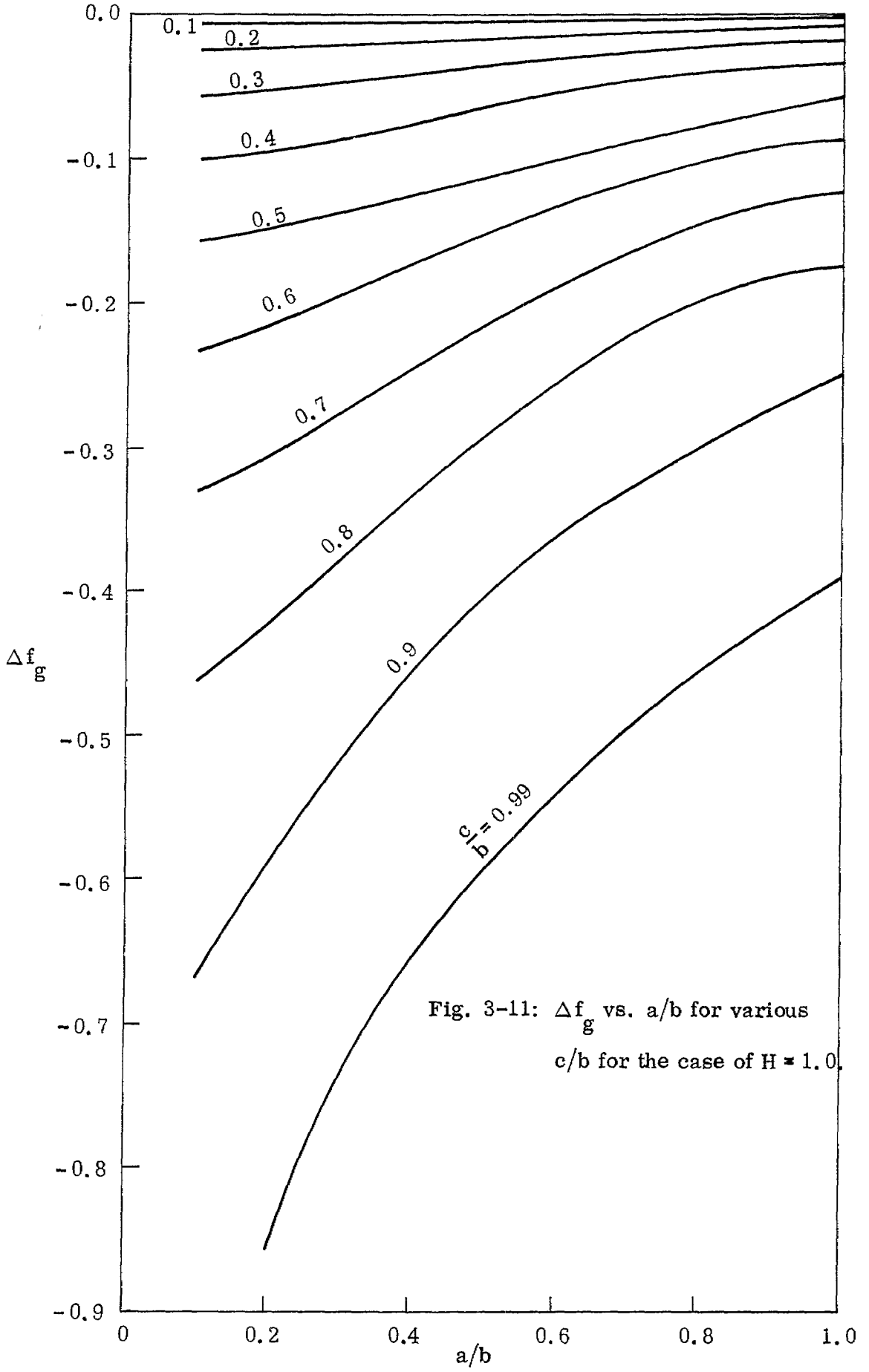

Fig. 3-11: Δf_g vs. a/b for various c/b for the case of H = 1.0

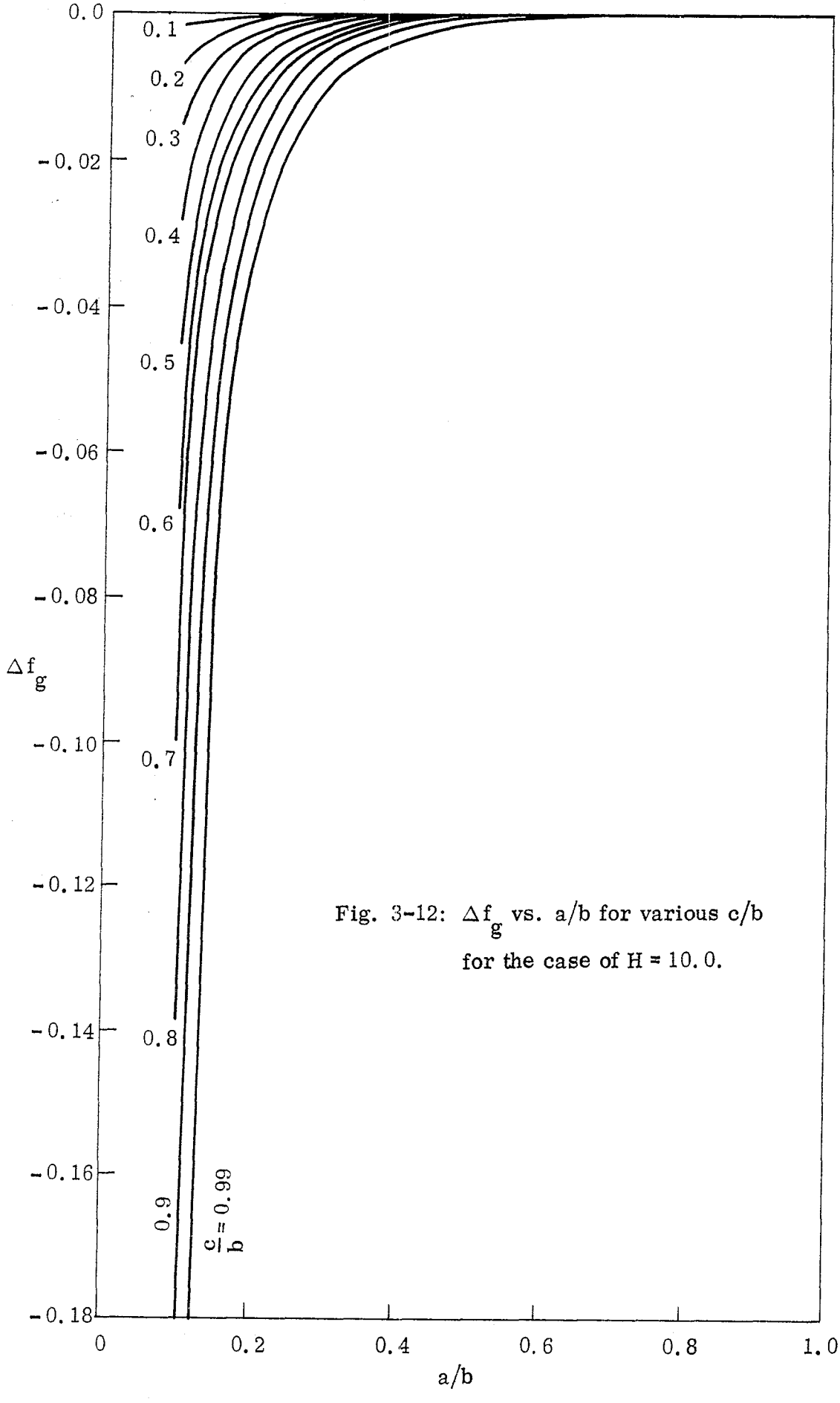

Fig. 3-12: Δf_g vs. a/b for various c/b for the case of H = 10.0.

Figures 3-13 through 3-15 show the variation of charge densities on circular cylinders for the cases mentioned previously. ϕ indicated in each figure corresponds to θ in the work of Latham. It is to be noted that, due to the normalization in the computation, the actual charge density is equal to $\frac{V_o a}{2\pi\epsilon_o}$ times the values given in these figures.

Table VII: Fourier coefficients A_n for charge density on the circular cylinder with H = 0.

a/b = 0.1

A_n / c/b	A_1	A_3	A_5	A_7
0.1	-0.0172			

a/b = 0.2

A_n / c/b	A_1	A_3	A_5	A_7
0.1	-0.0418			
0.2	-0.0427	+0.0016		

a/b = 0.5

A_n / c/b	A_1	A_3	A_5	A_7
0.2	-0.140			
0.5	-0.168	+0.006		
0.99	-0.452	+0.077	-0.01	

a/b = 1.0

A_n / c/b	A_1	A_3	A_5	A_7	A_9	A_{11}	A_{13}	A_{15}
0.1	-0.31							
0.2	-0.318							
0.4	-0.354	+0.0018						
0.6	-0.438	+0.015						
0.8	-0.667	+0.1	-0.01	+0.022				
0.9	-1.03	+0.32	-0.085	+0.029	-0.011	+0.003		

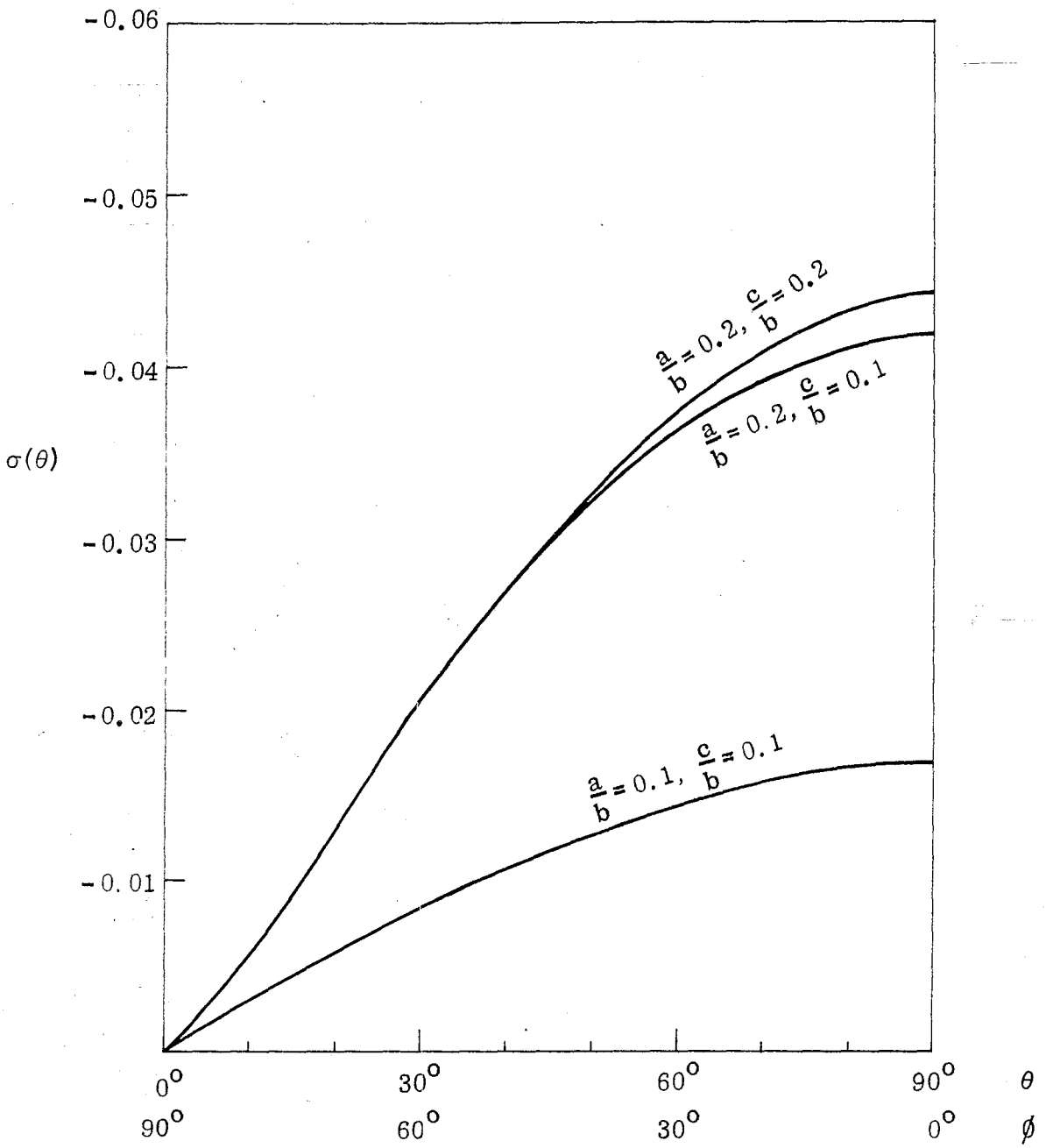

Fig. 3-13: $\sigma(\theta)$ for $\frac{a}{b} = 0.1$, $\frac{c}{b} = 0.1$ and $\frac{a}{b} = 0.2$, $\frac{c}{b} = 0.1, 0.2$, $\frac{h}{a} = 0.$

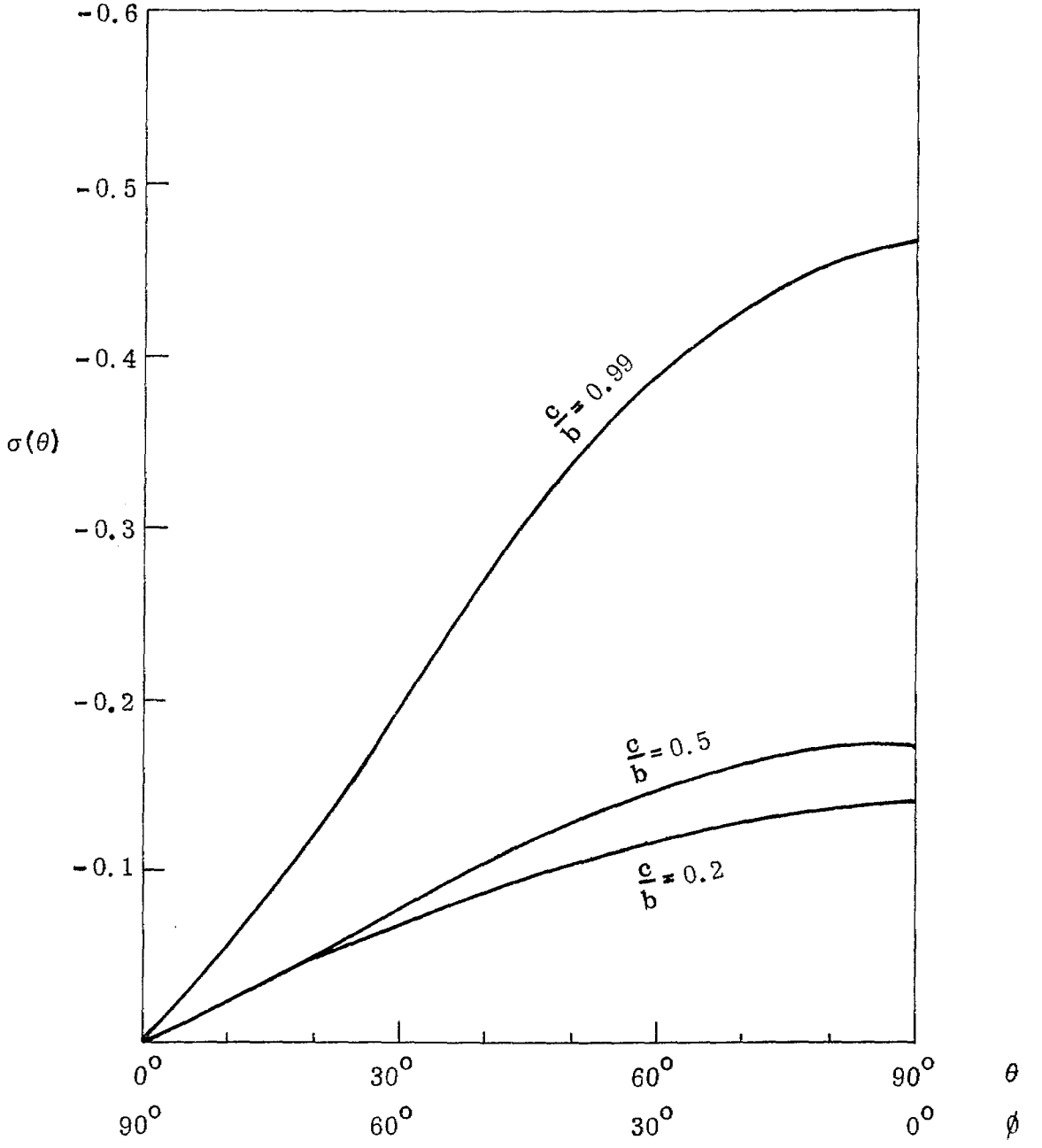

Fig. 3-14: $\sigma(\theta)$ for $\frac{a}{b} = 0.5$, $\frac{c}{b} = 0.2,\ 0.5,\ 0.99$, $\frac{h}{a} = 0$.

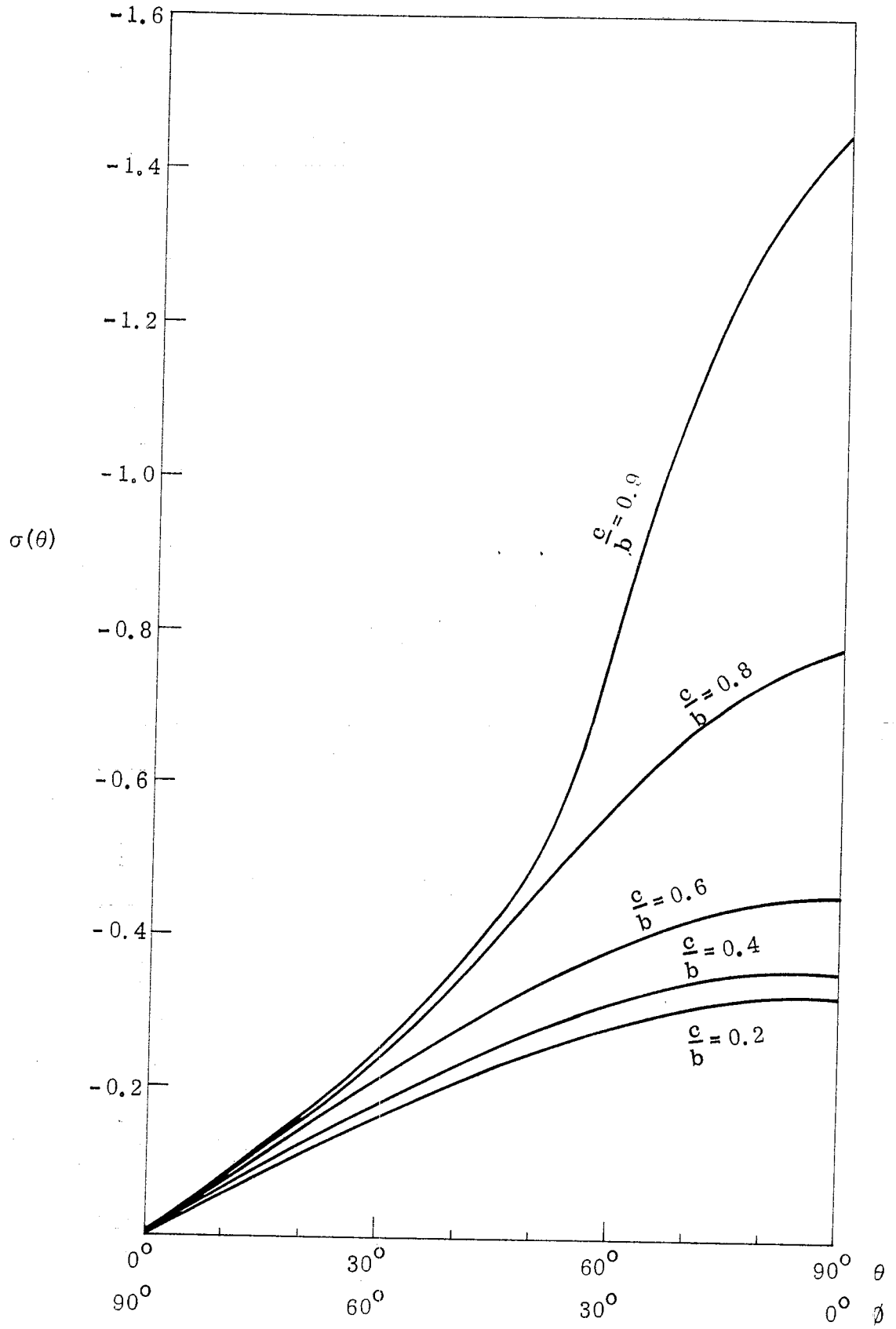

Fig. 3-15: $\sigma(\theta)$ for $\frac{a}{b} = 1.0$, $\frac{c}{b} = 0.2,\ 0.4,\ 0.6,\ 0.8$, $\frac{h}{a} = 0.$

IV

CONCLUSIONS

Based on the numerical results presented in Section III, the following qualitative observations can be made for the effect of the presence of a circular cylinder within two parallel plates of finite width on the impedance of the system and charge density of the circular cylinder. It is to be noted that the charge density on the cylinder is computed only for the case of $\frac{h}{a} = H = 0$.

(a) The presence of a circular cylinder, for all $\frac{h}{a} < \infty$, decreases the impedance of the system from that of the system without the cylinder.

(b) With the position of the cylinder fixed, as its radius increases, the impedance of the system decreases somewhat in an exponential fashion.

(c) For all radii of the cylinders within the limit $0 < \frac{c}{b} < 1$ and for all $\frac{a}{b}$ considered in this report the lowering of impedance of the system due to the presence of the cylinder is maximum at $\frac{h}{a} = 0$.

(d) For the fixed radius of the cylinder, the lowering effect of impedance by the cylinder becomes less as $\frac{a}{b}$ increases.

(e) For all $\frac{c}{b}$ $(0 < \frac{c}{b} \leq \frac{a}{b})$ considered, $\sigma(\theta)$ increases with $\frac{a}{b}$.

(f) $\sigma(\theta)$ is always maximum at $\theta = 90^{o}$.

(g) With $\frac{a}{b}$ fixed, as $\frac{c}{b}$ increases to $1 - \delta$, where $\delta > 0$ are small, $\sigma(\theta)$ increases sharply as θ approaches 90^{o}.

V

REFERENCES

(1) C-M. Chu, S. K. Cho, Sensor and Simulation Note 161, "Field Distribution for Parallel Plate Transmission Line of Finite Width in Proximity to a Conducting Plane," November 1972.

(2) R. W. Latham, Sensor and Simulation Note 55, "Interaction Between a Cylindrical Test Body and a Parallel Plate Simulator," May 1968.

(3) T. L. Brown and K. D. Granzow, Sensor and Simulation Note 52, "A parameter study of two Parallel Plate Transmission Line Simulators of EMP Sensor and Simulation Note 21," April 1968.

APPENDIX A

Charge Distribution on the Cylinder

In this Appendix, the algebraic steps leading from Eq. (15) to Eq. (16), concerning the charge density on the cylinder, are outlined.

In Eq. (15)

$$\frac{\partial \phi}{\partial r} + i \frac{\partial \psi}{\partial r} = \frac{1}{2\pi\epsilon_o} \int_{h-a}^{h+a} dx' \sigma(x') \left[\frac{1}{re^{i\theta} - x' + ib} + \frac{1}{re^{i\theta} - \frac{c^2}{x' - ib}} - \frac{1}{re^{i\theta} - x' - ib} - \frac{1}{re^{i\theta} - \frac{c^2}{x' + ib}} \right] e^{i\theta} . \qquad (A-1)$$

If we let $r \to c$, each term in the integrand of (A-1) may be written as:

$$\lim_{r \to c} \frac{e^{i\theta}}{re^{i\theta} - x' + ib} = -\frac{e^{i\theta}}{x' - ib - ce^{i\theta}} , \qquad (A-2)$$

$$\lim_{r \to c} \frac{-e^{i\theta}}{re^{i\theta} - x' - ib} = \frac{e^{i\theta}}{x' + ib - ce^{i\theta}} , \qquad (A-3)$$

$$\lim_{r \to c} \frac{e^{i\theta}}{re^{i\theta} - \frac{c^2}{x' - ib}} = \frac{\frac{1}{c}(x' - ib)}{(x' - ib) - ce^{-i\theta}} = \frac{1}{c} + \frac{e^{-i\theta}}{(x' - ib) - ce^{-i\theta}} , \qquad (A-4)$$

$$\lim_{r \to c} \frac{-e^{i\theta}}{re^{i\theta} - \frac{c^2}{x' + ib}} = \frac{-\frac{1}{c}(x' + ib)}{(x' + ib) - ce^{-i\theta}} = -\frac{1}{c} - \frac{e^{-i\theta}}{(x' + ib) - ce^{-i\theta}} . \qquad (A-5)$$

Introducing these into Eq. (A-1) yields

$$\left(\frac{\partial \phi}{\partial r} + i\frac{\partial \psi}{\partial r}\right)_{r=c}$$

$$= \frac{1}{2\pi\epsilon_o}\int_{h-a}^{h+a} \sigma(x')\,dx' \left[\frac{e^{i\theta}}{x' + ib - ce^{i\theta}} + \frac{e^{-i\theta}}{x' - ib - ce^{-i\theta}} - \frac{e^{i\theta}}{x' - ib - ce^{-i\theta}} - \frac{e^{-i\theta}}{x' + ib - ce^{-i\theta}}\right] . \tag{A-6}$$

Equation (A-6) reveals that

$$\left.\frac{\partial \psi}{\partial r}\right|_{r=c} = 0 .$$

Introducing the normalized quantities,

$$x' = as + h = a(s + H)$$

$$x' \pm ib = a\left(s + H \pm i\frac{B}{2}\right)$$

and

$$C = \frac{c}{a}$$

into (A-6), we have:

$$\sigma(\theta) = -\left.\frac{\partial \phi}{\partial r}\right|_{r=c} \epsilon_o$$

$$= -\frac{1}{2\pi}\int_{-1}^{1} \sigma(s)\,ds \left[\frac{e^{i\theta}}{s + H + i\frac{B}{2} - Ce^{i\theta}} + \frac{e^{-i\theta}}{s + H - i\frac{B}{2} - Ce^{-i\theta}} - \right.$$

$$\left. - \frac{e^{i\theta}}{s + H - i\frac{B}{2} - Ce^{i\theta}} - \frac{e^{-i\theta}}{s + H + i\frac{B}{2} - Ce^{-i\theta}}\right] . \tag{A-7}$$

Using the relation

$$\frac{e^{\pm i\theta}}{s + H \pm i\frac{B}{2} - Ce^{\pm i\theta}} = \sum_{n=1}^{\infty} \frac{C^{n-1} e^{\pm jn\theta}}{(s + H \pm i\frac{B}{2})x} , \tag{A-8}$$

we may reduce Eq. (A-7) to

$$\sigma(\theta) = -\frac{i}{\pi}\int_{-1}^{1}\sigma(s)\,ds\sum_{n=1}^{\infty}C^{n-1}\left[\frac{1}{(s+H+i\frac{B}{2})n} - \frac{1}{(s+H-i\frac{B}{2})n}\right]\sin n\theta \quad . \qquad \text{(A-9)}$$

This is Eq. (16) in the text.